JACS
JOURNAL OF THE AMERICAN CHEMICAL SOCIETY

ARTICLE

pubs.acs.org/JACS

C−C Activation in the Solid State in an Organometallic σ-Complex

Adrian B. Chaplin, Jennifer C. Green, and Andrew S. Weller*

Inorganic Chemistry Laboratory, Department of Chemistry, University of Oxford, South Parks Road, Oxford OX1 3QR, U.K.

Supporting Information

ABSTRACT: Herein is reported the synthesis, by a solid-state reaction from $[Ir(NBD)_2(P^iPr_3)][BAr^F_4]$, of the first example of a C−C σ-complex with iridium, $[Ir(BINOR\text{-}S)(P^iPr_3)][BAr^F_4]$. This compound is unique in that in the solid state it undergoes reversible activation of the C−C single bond that interacts with the metal center, establishing a temperature-dependent equilibrium between Ir(III) C−C σ/Ir(V) bis-alkyl complexes. This process has been interrogated by variable-temperature X-ray diffraction, NMR spectroscopy, and DFT calculations.

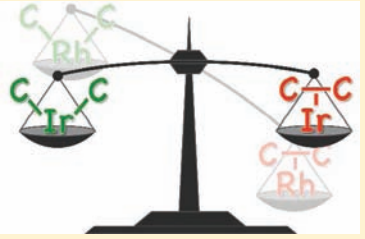

INTRODUCTION

The coordination chemistry of transition-metal centers with saturated bonds, such as dihydrogen (H−H), alkanes (C−H), silanes (Si−H), and boranes (B−H), is of significant interest with regard to their fundamental structures and bonding, activation, and subsequent utilization in chemical synthesis.[1−3] These so-called σ-complexes are prototypically defined by the coordination chemistry of the simplest member of the family, H_2, as reported in 1984 by Kubas.[4] Related intermolecular M···H−C bonds, i.e., alkane complexes, are scarce and metastable in solution,[5−7] while intramolecular agostic M···H−C complexes are much better represented.[2] The analogous M···C−C σ-complexes (intra- or intermolecular) are of considerable interest with regard to the cleavage and formation of carbon−carbon bonds using transition metals,[8−12] processes of significant relevance to organic synthesis and petroleum research. Despite this, examples of M···C−C σ-complexes are rare compared to M···HC, and limited to intramolecular systems,[13−26] as kinetically such complexes are disfavored due to the relative inaccessibility and orbital directionality associated with the C−C bond compared with C−H.[8] We recently reported the synthesis of a rhodium complex with a well-defined intramolecular σ-C−C interaction, $[Rh(BINOR\text{-}S)(P^iPr_3)][BAr^F_4]$ (**1**, BINOR-S = 1,2,4,5,6,8-dimetheno-*S*-indacene and $Ar^F = C_6H_3(CF_3)_2$).[27,28] This complex has a $\{Rh(P^iPr_3)\}^+$ fragment coordinated to a saturated organic ligand (BINOR-S) through a metallacyclobutane ring and σ-C−C interaction from a cyclopropane unit (Scheme 1). There is also a C−H···Rh agostic interaction.

σ-Complexes are particularly interesting as they represent intermediates in the activation of strong covalent bonds by oxidative cleavage (Scheme 1).[1,3] For example, in the now classic study by Kubas, interconverting tautomers of $W(PCy_3)_2(CO)_3H_2$ were found to exist: a W(II)−dihydride, the product of oxidative cleavage, and a W(0)−dihydrogen σ-complex.[4] Equilibrium mixtures between σ-alkane and alkyl hydride complexes have also been observed in alkane complexes of the $\{Re(\eta^5\text{-}C_5H_5)(CO)(PF_3)\}$ fragment.[5] Whether oxidative cleavage

Scheme 1. (a) Representation of the Transition-Metal-Mediated Activation of σ-Bonds and (b) Structure of $[Rh(BINOR\text{-}S)(P^iPr_3)][BAr^F_4]$ (1)

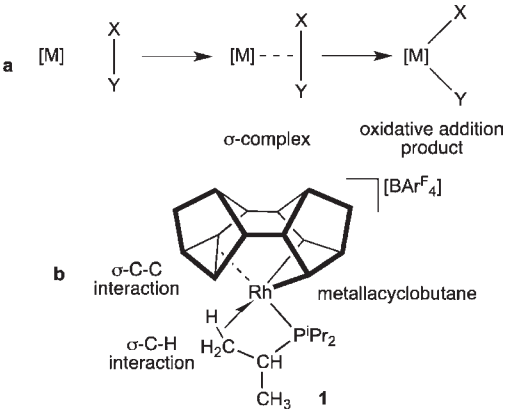

of the σ-bound ligand occurs or not can be controlled by the relative position of the transition metal in a particular triad, among other factors;[29] heavier congeners with their energetically more accessible higher oxidation states can favor the products of oxidative cleavage. For example, $[Rh(\eta^5\text{-}C_5Me_5)(PMe_3)H(H_2)][BAr^F_4]$ is formulated as a Rh(III) hydride/dihydrogen complex,[30] while $[Ir(\eta^5\text{-}C_5Me_5)(PMe_3)H_3][BF_4]$ is an Ir(V) trihydride.[31] Recently, Brookhart, Goldberg, and co-workers demonstrated similar behavior in methane complexes of the group 9 $\{M(2,6\text{-}(^tBu_2PO)_2C_5H_3N)\}^+$ (M = Rh, Ir) fragments. The rhodium complex is a σ-methane Rh(I) species,[7] while the iridium complex is an Ir(III) hydrido-methyl (albeit in fast self-exchange via a proposed Ir(I) σ-methane complex).[32] As σ-C−C

Received: May 24, 2011
Published: July 07, 2011

Scheme 2. Formation of $[Ir(BINOR\text{-}S)(P^iPr_3)][BAr^F{}_4]$ (3)

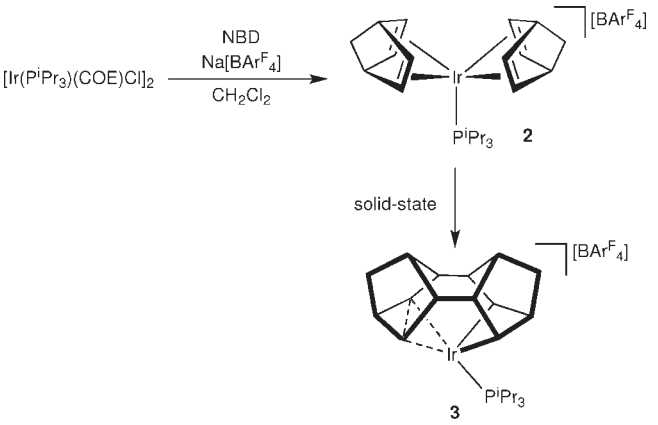

complexes are rare, such an isomeric pair has yet to be observed for analogous carbon−carbon bonds.

The existence of such isomers is suggested on the basis of experimental and computational investigations on **1**.[27,28] Using NMR spectroscopy, it was shown that this Rh(III) complex undergoes rapid reversible C−C oxidative cleavage/reductive coupling on the NMR time scale in solution. The calculated mechanism invoked a putative Rh(V) alkyl intermediate: the product of activation of the σ-C−C bond. Although this dynamic process can be arrested at low temperature in solution,[27,28] allowing the barrier to be determined, the key Rh(V) intermediate remains elusive. In order to realize the synthesis of such an intermediate, we targeted the synthesis of the Ir congener to **1**, hoping to exploit the more accessible (V) oxidation state of iridium compared to rhodium. To this end, we now report the synthesis of $[Ir(BINOR\text{-}S)(P^iPr_3)][BAr^F{}_4]$ (**3**), in which both the Ir(III) σ-complex and Ir(V) oxidative cleavage products coexist in the solid state. We find that these two complexes are in equilibrium with one another, and the position of the equilibrium can be adjusted by changing the temperature. Although reversible C−C activation has been reported previously[28,33−35] and σ-bound complexes have been implicated in such processes,[28,36,37] the observation of intimately connected σ and oxidative cleavage product complexes is, we believe, unknown.

RESULTS AND DISCUSSION

The precursor complex $[Ir(NBD)_2(P^iPr_3)][BAr^F{}_4]$ (**2**, NBD = 2,5-norbornadiene) was prepared by reaction of excess NBD and $Na[BAr^F{}_4]$ with $[Ir(COE)(P^iPr_3)Cl]_2$ (COE = cyclooctene) in CH_2Cl_2, as shown in Scheme 2. By comparison, the Rh congener of **2** cannot be observed, as it presumably proceeds immediately to form **1**.[27] Complex **2** is isolated as an air- and temperature-sensitive crystalline material. The solid-state structure of the cation, which is best described as having a distorted square-based pyramidal geometry, is shown in Figure 1. The structure of a PMe_3 analogue of **2**, $[Ir(NBD)_2(PMe_3)]^+$ (**2′**), has recently been calculated and shows very similar structural metrics.[38] The overall barrier to dimerization of the coordinated NBD units to form BINOR-S in **2′** was also calculated and was shown to be 123.9 kJ mol^{-1}, significantly higher than that for the rhodium analogue (92.4 kJ mol^{-1}) and consistent with our experimental observations. Although complex **2** can be isolated,

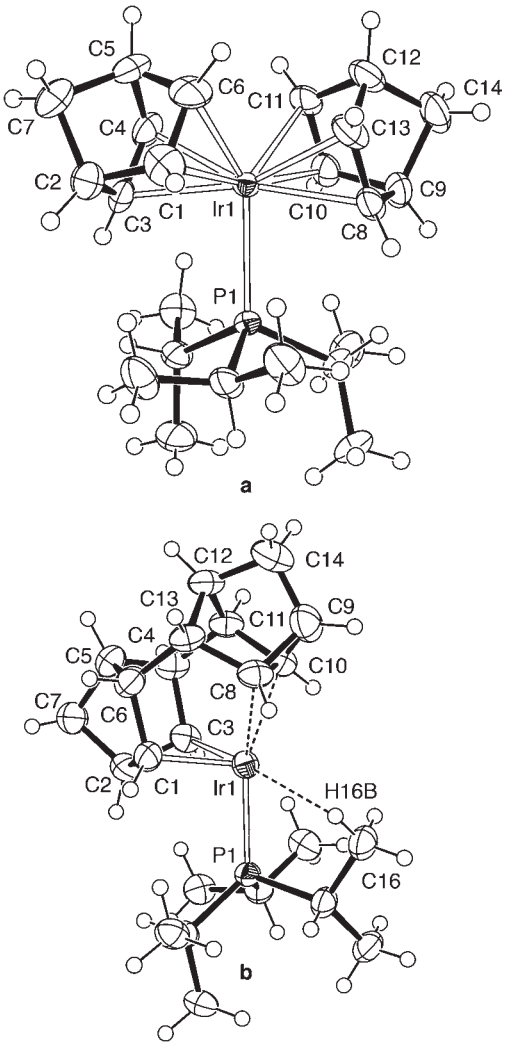

Figure 1. Molecular structures of **2** (a) and **3** (b): ORTEP plots with thermal ellipsoids drawn at the 50% probability level. Data were collected at 150 K. The structure of **3** presented here is refined without cation disorder modeling (see text). Anions and solvent molecules are omitted for clarity. Selected bond distances (Å) for **2**: Ir1−P1, 2.4768(8); Ir1−C1, 2.190(4); Ir1−C6, 2.169(4); Ir1−C3, 2.275(3); Ir1−C4, 2.250(4); Ir1−C8, 2.254(3); Ir1−C13, 2.237(4); Ir1−C10, 2.225(3); Ir1−C11, 2.192(3). Selected parameters for **3** are listed in Table 1.

in CD_2Cl_2 solution it proceeds slowly to form $[Ir(BINOR\text{-}S)(P^iPr_3)][BAr^F{}_4]$ (**3**) alongside decomposition to unidentified products (see Supporting Information). Complex **3** is itself unstable in solution at room temperature (half-life of 5.3 ± 0.2 h), decomposing to give multiple products including free BINOR-S. This stability profile is similar to that of the Rh congener **1**, which decomposes in CH_2Cl_2 over 24 h. Thus, although the formation of **3** can be observed by NMR spectroscopy, its low stability means that its isolation as a pure material using solution techniques is problematic. To circumvent this, we carried out the synthesis of **3** in the *solid state* by reaction of **2** at 40 °C to afford pure **3** after 20 h in quantitative yield. Monitoring this reaction over a range of temperatures using NMR spectroscopy (samples analyzed in CD_2Cl_2 solution, see Supporting Information) showed a reaction profile that fitted zero-order reaction kinetics[39] with activation parameters of $\Delta H^{\ddagger}$ = 106.2 ± 1.1 kJ mol^{-1} and

Table 1. Selected Distances (Å) and Angles (°) for the Structures of 1 and 3 at Different Temperatures[a]

	1		3		
	100 K	250 K	100 K	250 K	150 K
cation structure	ordered	ordered	disordered, not modeled	disordered, not modeled	disordered, two-component model (**3a**, **3b**)
M−P1	2.2711(5)	2.2718(10)	2.2884(8)	2.3545(15)	2.3191(9)
M−C8	2.368(2)	2.369(4)	2.305(3)	2.220(6)	2.26(2),[b] 2.27(4)[c]
M−C10	2.356(2)	2.359(4)	2.294(3)	2.206(8)	2.284(9),[b] 2.18(2)[c]
C8−C10	1.610(3)	1.609(7)	1.704(5)	1.833(13)	1.645(7),[b,d] 2.069(8)[c,d]
C8−C9−C10	64.32(15)	64.4(3)	68.4(2)	76.3(7)	66.6(6),[b] 82.7(14)[c]
M−C1	2.043(2)	2.033(4)	2.061(3)	2.046(7)	2.057(4)
M−C3	2.036(2)	2.028(4)	2.050(3)	2.043(7)	2.045(4)
C1−C2−C3	91.80(16)	92.3(3)	92.4(3)	92.3(6)	92.3(3)
M−C16	2.906(2)	2.921(5)	2.955(4)	3.004(9)	2.970(5)

[a] See Supporting Information for complete listing of structural parameters. [b] Parameters associated with disordered component **3a** only. [c] Parameters associated with disordered component **3b** only. [d] These parameters are restrained directly (see main text).

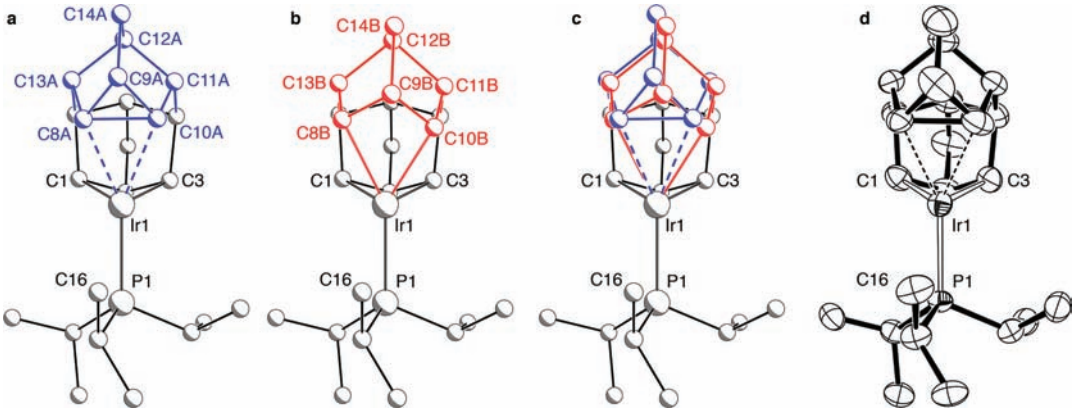

Figure 2. Disorder models for the molecular structure of **3**: ball-and-stick representations of the individual disordered components **3a** (a) and **3b** (b), the combined model (c), and an ORTEP plot (thermal ellipsoids drawn at the 50% probability level) of **3** refined without cation disorder modeling (d). Anions and hydrogen atoms are omitted for clarity. Data were collected at 150 K.

$\Delta S^{\ddagger} = +6 \pm 4$ J mol^{-1} K^{-1}. $\Delta G^{\ddagger}(298\text{ K}) = 104 \pm 2$ kJ mol^{-1}, comparing well with that calculated for the equivalent process involving **2′** (123.6 kJ mol^{-1}).[38] Crystals suitable for an X-ray diffraction experiment were grown at low temperature (243 K, CH_2Cl_2/pentane) in an argon-filled glovebox. In the solid state **3** is extremely sensitive and is unstable outside a purified Ar or vacuum atmosphere, decomposing rapidly. The dimerization of NBD on group 9 metals has been reported previously.[40−42]

Solution $^{31}P\{^1H\}$ NMR data for **3** show a single, sharp, signal over the temperature range from 298 to 200 K (CD_2Cl_2) that moves significantly to lower frequency on cooling (δ 47.2 at 298 K; δ 36.2 at 200 K). By contrast, **1** shifts by only 1.8 ppm over the same temperature range.[27] For **3**, local C_{2v} symmetry is observed for the BINOR-S ligand by ^1H and $^{13}C\{^1H\}$ NMR spectroscopy, even on cooling to 200 K. As for the $^{31}P\{^1H\}$ NMR spectrum, changes in chemical shift with temperature are also observed. These NMR data suggest a rapid, time-averaged, fluxional process that makes the two sides of the BINOR-S ligand equivalent, by movement of the phosphine from one side of the molecule to the other, as in the solid state the ligand has only C_s symmetry. For **1**, we have previously shown that this process can be frozen out (200 K, $\Delta G^{\ddagger}(298\text{ K}) = 44.8 \pm 4$ kJ mol^{-1}) to reveal solution NMR data fully consistent with the solid-state structure, and calculations suggest a C_s-symmetric Rh(V) intermediate.[28] For **3**, the barrier to this process must be considerably lower. The changes with temperature observed by NMR spectroscopy for **3** suggest a change in population between chemically distinct species that are in rapid equilibrium with one another.

The solid-state structure of **3** was determined by X-ray diffraction over a wide temperature range (100−250 K; see Figure 1 for the 150 K structure), and the key structural metrics that arise from these experiments are presented in Table 1. Analysis of these data suggests an apparent lengthening of the σ-C−C distance with temperature [C8−C10, 1.704(5) Å at 100 K, 1.833(13) Å at 250 K], alongside a concomitant apparent lengthening of the Ir1−P1 bond [2.2884(8) Å at 100 K, 2.3545(15) Å at 250 K]. The metrics associated with the metallacyclobutane (Ir,C1,C2,C3) and C−H···Ir agostic interaction (Ir1−C16) do not change significantly. These data suggest increasing activation of the C−C σ-bond with temperature and that these structural changes are localized primarily to one part of the molecule. Repeating these measurements on a different crystalline sample, using a different diffractometer, and cycling the temperature (cooling from 250 to 100 K, followed by warming to 250 K) on the same sample all gave the same results.

The behavior observed for **3** in the solid state is rationalized using a crystallographic disorder model involving a mixture of two cationic components in the crystal lattice (Figure 2), the relative ratio of which changes with temperature, resulting in apparent changes in the C8−C10, Ir1−C8, Ir1−C10, and Ir1−P1 distances. The main disordered component is an Ir(III) σ-C−C complex, **3a**, that is isostructural with its Rh congener **1**. In this structure there is a metallacyclobutane (Ir,C1,C2,C3) and a cyclopropane moiety (C8A,C9A,C10A) that adopts a σ-C−C interaction with the metal center. The other component, **3b**, has two metallacyclobutane units (Ir1,C1,C2,C3 and Ir1,C8B,C9B, C10B) and a formal Ir(V) oxidation state. The phosphine ligand and supporting C−H···Ir agostic interaction (Ir1−C16) are common to both components. These two isomers, **3a** and **3b**, were modeled by restraining the C8−C10 distance in **3a** and **3b** to 1.64 and 2.07 Å, respectively, distances that were suggested by DFT calculations (see below) and are crystallographically and chemically sensible for an activated cyclopropane and a metallacyclobutane respectively.[27,28,37] Similar progressive changes in bond length with temperature that are modeled using a temperature-dependent population change between two disordered isomers have been observed for Fe−cyanide spin-crossover complexes, where the Fe−N bonds show a systematic increase with increasing temperature due to a change in the weighted average of two different Fe−N environments, in this case on moving from a low-spin to a high-spin electronic configuration.[43] Data collections on **1**, which notably crystallizes in the same space group as **3**, were repeated over the same temperature range. No statistically significant variation in any of the measured distances was found (Table 1). The unit cell volume changed by only 3.5% for both **1** and **3** over this temperature range. This demonstrates that the structural changes observed are due to the replacement of Rh (4d metal) with Ir (5d metal) on moving from **1** to **3**.

This structural change between **3a** and **3b** is thus formulated as a C−C oxidative cleavage of a σ-bound cyclopropane ring. Such a change from a σ-interaction (**3a**) to two Ir−C covalent bonds (**3b**) would be expected to have a pronounced effect on the *trans*-disposed phosphine group, owing to the large *trans*-influence of a bis-alkyl compared to a σ-C−C unit. Although the heavy phosphorus atom was not explicitly split in the disorder model this change is manifested in the apparent lengthening of the measured Ir1−P1 distance with temperature associated with the increase in the relative population of the Ir(V) isomer (Figure 2, Table 1).

That the relative populations of the two isomers **3a** and **3b** change reversibly with temperature shows that there is an equilibrium between the two disordered components. This is similar to the dynamic disorder[44] reported in the solid state for mixed $M_3(CO)_{12}$ clusters (M = Fe, Ru, Os).[45,46] In the solid state at 100 K, the **3a**:**3b** ratio is 83(2):17(2), which changes at 250 K to 55(2):45(2). A Van't Hoff plot (Figure 3) clearly demonstrates the change in the position of the equilibrium with temperature and yields the following thermodynamic parameters: $\Delta H = 1.93 \pm 0.03$ kJ mol^{-1}, $\Delta S = +6.2 \pm 0.2$ J mol^{-1} K^{-1}, and $\Delta G(298\ \text{K}) = +0.09 \pm 0.08$ kJ mol^{-1}. These data show the Ir(III) and Ir(V) complexes to be energetically very similar to one another. A similar analysis has been used to map the rotational progression of nitrosyl ligands in Fe−porphyrin complexes with temperature in the solid state.[47]

Further support for the description of the solid-state structure of **3** using a two-component model comes from significant

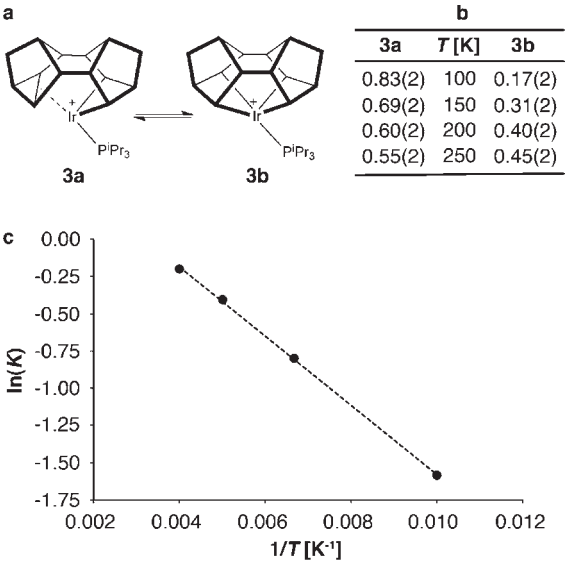

Figure 3. Solid-state dynamic behavior of **3**: reaction scheme demonstrating the structural change between the tautomers of **3** (a), populations of the tautomers at different temperatures determined using X-ray diffraction (b), and Van't Hoff plot for this process (c) (R^2(fit) = 0.999).

deviations from rigid-bond behavior for the C8−C10 and Ir1−P1 bonds when the cation of **3** is refined without using this model, indicating the presence of disorder (Hirshfeld rigid-bond test, see Supporting Information).[48] In contrast, the bonds not significantly involved in the structural change (i.e., Ir1−C1, Ir1−C3) do not show any similar signs of disorder. Importantly, no evidence of disorder is found across the complete temperature range for **1**, with C8−C10 and Rh1−P1 bonds notably showing good rigid-bond behavior. We are thus confident that this variation in C8−C10 and Ir1−P1 bond distances with temperature in **3** is a consequence of a reversible intramolecular change in bonding and that this does not happen to any significant degree for the Rh analogue.

As X-ray diffraction gives only the average of all possible atomic displacements in the entire crystal on the time scale of the X-ray experiment (i.e., hours),[44] to probe this dynamic change further we have obtained the solid-state $^{31}P\{^1H\}$ MAS−NMR spectra of **1** and **3** over a variable-temperature range (298 to 213 K); which gives information on the NMR time scale (seconds) regarding local atomic environments. For **3**, a single peak is observed that progressively shifts from δ 35.2 (298 K) to δ 29.9 (213 K), mirroring that observation in solution. The signal broadens upon cooling (fwhm 260 vs 320 Hz). These observations (albeit not covering the same range as for the X-ray diffraction experiments) are indicative of a weighted average chemical shift of two chemically distant species that are in dynamic equilibrium with one another and suggest that the barrier to interconversion in the solid state between **3a** and **3b** is low, as might be expected for such a simple process that does not involve major atomic reorganization. These changes are reversible upon warming to 298 K, as for the X-ray experiments. Higher temperatures resulted in the onset of decomposition. For **1**, a single peak is observed at δ 46.7 [J(RhP) = 208 Hz] that, as in solution, shifts by a significantly lesser degree upon cooling to 213 K compared to **3**, to δ 44.5 [J(RhP) = 220 Hz]. At room temperature, the signal becomes broader (fwhm 80 vs 140 Hz). These results are consistent with a higher barrier to

dx.doi.org/10.1021/ja2047599 |*J. Am. Chem. Soc.* 2011, 133, 13162–13168

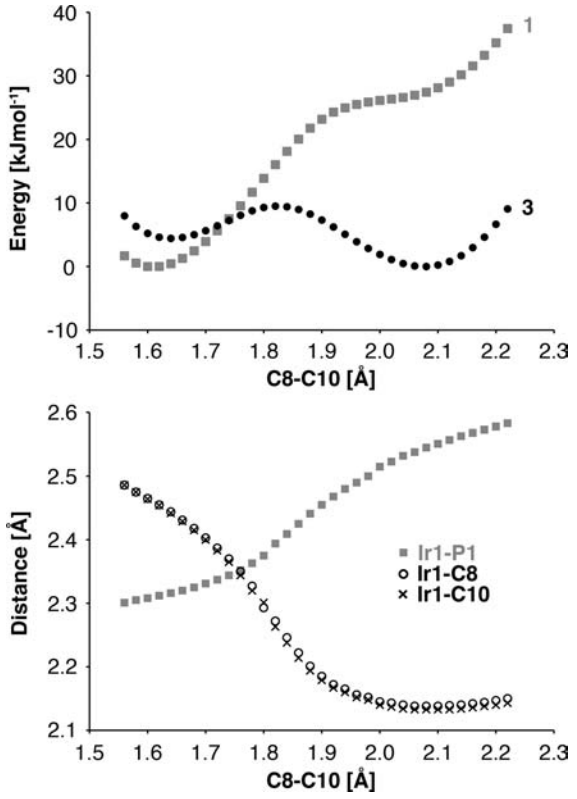

Figure 4. Calculated potential energy surface for C−C bond activation in **1** and **3**: SCF energy with changes in C8−C10 bond distance for **1** and **3** and correlations between the C8−C10, Ir1−P1, Ir1−C8, and Ir1−C10 bond distances during this process.

interconversion in **1** than in **3**. Unlike in solution, where the phosphine ligand would be free to move during the fluxional process, making each side of the BINOR-S fragment equivalent on the NMR time scale (i.e., time-averaged C_{2v} symmetry), in the solid state this is not possible due to the constraints imposed by the lattice, and the molecule would retain approximate C_s symmetry.

DFT calculations[49] were able to identify two minima for **3**, one with a C8−C10 bond length of 1.64 Å (**3a**) and the other 2.07 Å (**3b**), corresponding to, and fully consistent with, the inferred structures of **3a** (Ir(III)) and **3b** (Ir(V)). Similarly, the calculated structure of **1** shows excellent agreement with the observed (static) structure of **1** in the solid state [e.g., C8−C10, 1.61 Å (calc) versus 1.610(3) Å (100 K)]. That the calculated C−C sigma bond in **3a** is longer than in **1** (1.64 versus 1.61 Å, respectively) suggests a greater degree of C−C activation in **3a** and underscores that these structural changes are due to the move from a 4d to a 5d metal. It also parallels the activation, but not scission, of dihydrogen when bound to different metal centers in stretched dihydrogen complexes.[1] The SCF energy of **3a** was found to be 4 kJ mol^{-1} higher than that of **3b** with an enthalpy change ΔH^0(298 K) = −10 kJ mol^{-1}, in satisfactory agreement with the small energy difference found experimentally, though of the wrong sign. A transition state was identified between the two species, with activation free energies of 4 kJ mol^{-1} from **3a** and 11 kJ mol^{-1} from **3b**.[50] This low barrier is consistent with the results of the solid-state NMR experiments. The C8−C10 distance in the transition state was 1.82 Å. A scan of the SCF energy with changing C8−C10 bond length is shown in Figure 4; two minima are clearly evident. For **1**, a similar scan showed a point of inflection at long C−C distances in a steadily rising curve, which is related to the Rh(V) transition state for the fluxional process for the BINOR-S ligand in solution.[28] There is also a strong correlation of the C8−C10 distance with the changes in Ir1−P1, Ir1−C8, and Ir1−C10 bond lengths for **3**. As the C−C distance increases, the phosphine is also found to tilt slightly to one side. All these trends are fully consistent with the structural variation observed by X-ray diffraction at different temperatures, and the steeper potential energy curve associated with the C−C distance in **1** underscores the observation that the Rh(III) oxidation state is preferred in the solid state, reflecting the relative inaccessibility of the Rh(V) oxidation state.[51] Examination of the frontier orbitals (Supporting Information) of **3a** and **3b** showed that, while **3a** has three occupied orbitals principally of d character and two unoccupied orbitals, for **3b** the reverse is true, with two d orbitals being occupied in this case and three unoccupied.

CONCLUSIONS

We report here experimental and computational evidence that an Ir(III) σ-complex and an Ir(V) oxidative cleavage product coexist in the solid state. These two complexes are in equilibrium with one another, with the position of the equilibrium can be adjusted by changing the temperature. Related temperature-dependent behavior of isomeric (tautomeric) forms of bound σ complexes has previously been observed in solution for dihydrogen complexes. Pons and Heinekey reported a marked temperature dependence of J(HD) in isotopomers of [Ir(dmpm)-(η^5-C_5Me_5)H_2][$B(C_6F_5)_4$]$_2$ (dmpm = bis(dimethylphosphino)-methane), attributed to a rapidly established equilibrium between an Ir(III) dihydrogen complex and an Ir(V) *cis*-dihydride tautomer. That higher temperatures resulted in increased J(HD) values was interpreted as corresponding to an increased population of the dihydrogen isomer,[52,53] which was supported by computational work.[54−56] Saliently, the Rh congener [Rh-(dmpm)(η^5-C_5Me_5)H_2][$B(C_6F_5)_4$]$_2$ is formulated as a conventional Rh(III) dihydrogen analogue.[54] The similarity with the C−C σ-complexes **1** and **3** is thus striking and further strengthens our interpretation that both an Ir(III) σ-C−C complex and the corresponding Ir(V) C−C oxidative cleavage product are present in the solid state for **3** but not for **1**. If we take this view, **3** completes the series for σ coordination and reversible activation of the most important element−element σ-bonds with transition metal centers: H−H, C−H, and C−C.

EXPERIMENTAL SECTION

[Ir(NBD)$_2$(P^iPr_3)][BAr^F_4] (2). To a Schlenk flask charged with [Ir(COE)(P^iPr_3)Cl]$_2$[57] (0.200 g, 0.201 mmol) and Na[BAr^F_4] (0.365 g, 0.412 mmol) was added a solution of NBD (0.2 mL, 2 mmol) in CH_2Cl_2 (5 mL). The resulting suspension was stirred at room temperature for 30 min and then filtered. The crude product was precipitated by addition of excess hexane and isolated by filtration. Two successive recrystallizations from CH_2Cl_2/hexane gave the pure product as a cream-white microcrystalline solid. Yield = 0.350 g (62%). The solid product was stored under argon at −32 °C.

Data for **2**: ^{1}H NMR (CD_2Cl_2, 500 MHz, 298 K, using X-ray labeling scheme) δ 7.70−7.74 (m, 8H, Ar^F), 7.56 (br, 4H, Ar^F), 4.29 (br, 2H, $H^{2/9}$), 4.14 (app q, J = 4 Hz, 4H, $H^{1/3/8/10}$), 3.55 (br, 2H, $H^{5/12}$), 3.48 (dt, $^3J_{PH}$ = 7.2 Hz, $^3J_{HH}$ = 3.8 Hz, 4H, $H^{4/6/11/13}$), 3.00 (app oct, J = 7 Hz, PCH), 1.37 (dd, $^3J_{PH}$ = 13.5 Hz, $^3J_{HH}$ = 7.2 Hz, Me), 0.96 (br m, 4H, $H^{7/14}$); ^{31}P{^{1}H} NMR (CD_2Cl_2, 202 MHz, 298 K) δ −0.7 (s); ^{13}C{^{1}H} NMR (CD_2Cl_2, 126 MHz, 298 K) δ 162.3 (q, $^1J_{BC}$ = 50 Hz,

Ar^F), 135.4 (s, Ar^F), 129.4 (qq, $^2J_{FC}$ = 32 Hz, $^3J_{BC}$ = 3 Hz, Ar^F), 125.2 (q, $^1J_{FC}$ = 272 Hz, Ar^F), 118.0 (sept, $^3J_{FC}$ = 4 Hz, Ar^F), 66.8 (d, $^4J_{PC}$ = 1 Hz, $C^{7/14}$), 47.9 (d, $^3J_{PC}$ = 2 Hz, $C^{5/12}$), 45.9 (d, $^2J_{PC}$ = 6 Hz, $C^{1/3/8/10}$), 45.4 (d, $^3J_{PC}$ = 2 Hz, $C^{2/9}$), 42.4 (d, $^2J_{PC}$ = 4 Hz, $C^{4/6/11/13}$), 29.3 (d, $^1J_{PC}$ = 20 Hz, PCH), 20.3 (s, Me).

[Ir(BINOR-S)(P^iPr_3)][BAr^F_4] (3). A solid sample of **2** (0.080 g, 0.057 mmol) was heated at 40 °C under argon for 20 h, resulting in quantitative formation of the product as an orange solid.

Data for **3** (higher temperature): ^{1}H NMR (CD_2Cl_2, 500 MHz, 298 K, using X-ray labeling scheme) δ 7.70−7.74 (m, 8H, Ar^F), 7.56 (br, 4H, Ar^F), 3.97 (br app t, J = 3 Hz, 4H, $H^{1/3/8/10}$), 3.53 (br app t, J = 5 Hz, 2H, $H^{2/9}$), 2.70 (second-order app oct, $J \approx 7$ Hz, 3H, PCH), 2.30 (br, 2H, $H^{5/12}$), 1.62 (br, 4H, $H^{4/6/11/13}$), 1.33 (obscured app t, J = 2 Hz, 4H, $H^{7/14}$), 1.32 (dd, $^3J_{PH}$ = 14.5 Hz, $^3J_{HH}$ = 7.2 Hz, Me); $^{31}P\{^1H\}$ NMR (CD_2Cl_2, 500 MHz, 298 K) 47.2 (s); $^{13}C\{^1H\}$ NMR (CD_2Cl_2, 126 MHz, 298 K) δ 162.3 (q, $^1J_{BC}$ = 50 Hz, Ar^F), 135.4 (s, Ar^F), 129.4 (qq, $^2J_{FC}$ = 32 Hz, $^3J_{BC}$ = 3 Hz, Ar^F), 125.2 (q, $^1J_{FC}$ = 272 Hz, Ar^F), 118.0 (sept, $^3J_{FC}$ = 4 Hz, Ar^F), 51.9 (s, $C^{2/9}$), 46.9 (s, $C^{4/6/11/13}$), 35.3 (d, $^4J_{PC}$ = 3 Hz, $C^{7/14}$), 34.1 (s, $C^{5/12}$), 29.1 (d, $^2J_{PC}$ = 8 Hz, $C^{1/3/8/10}$), 24.3 (d, $^1J_{PC}$ = 22 Hz, PCH), 20.4 (s, Me).

Data for **3** (lower temperature): ^{1}H NMR (CD_2Cl_2, 500 MHz, 200 K) δ 7.69−7.74 (m, 8H, Ar^F), 7.53 (br, 4H, Ar^F), 3.74 (br app t, J = 4 Hz, 4H, $H^{1/3/8/10}$), 3.24 (br app t, J = 5 Hz, 2H, $H^{2/9}$), 2.53 (app oct, J = 8 Hz, 3H, PCH), 2.14 (br, 2H, $H^{5/12}$), 1.55 (br, 4H, $H^{4/6/11/13}$), 1.24 (br, 4H, $H^{7/14}$), 1.20 (dd, $^3J_{PH}$ = 14.4 Hz, $^3J_{HH}$ = 7.2 Hz, Me); $^{31}P\{^1H\}$ NMR (CD_2Cl_2, 202 MHz, 200 K) δ 36.2 (s); ^{13}C NMR (CD_2Cl_2, 126 MHz, 200 K, selected data from HSQC) δ 49.7 ($^1J_{CH}$ = 160 Hz, $C^{2/9}$), 44.1 ($^1J_{CH}$ = 136 Hz, $C^{4/6/11/13}$), 34.7 ($^1J_{CH}$ = 134 Hz, $C^{7/14}$), 33.4 ($^1J_{CH}$ = 148 Hz, $C^{5/12}$), 26.0 ($^1J_{CH}$ = 163 Hz, $C^{1/3/8/10}$), 23.0 ($^1J_{CH}$ = 128 Hz, PCH), 19.2 ($^1J_{CH}$ = 126 Hz, Me).

Anal. Calcd for $C_{55}H_{49}BF_{24}IrP$ (1399.96 g mol^{-1}): C, 47.19; H, 3.53. Found: C, 47.57; H, 3.63.

■ ASSOCIATED CONTENT

Supporting Information. Full synthetic, crystallographic characterization, and computational details (^{1}H, ^{13}C, ^{31}P solution and solid-state NMR spectroscopy and details of the crystallography on **1** and **3**). This material is available free of charge via the Internet at http://pubs.acs.org. Crystallographic data have also been deposited with the Cambridge Crystallographic Data Centre under CCDC 802171−802186. These data can be obtained free of charge from The Cambridge Crystallographic Data Centre via www.ccdc.cam.ac.uk/data_request/cif.

■ AUTHOR INFORMATION

Corresponding Author
andrew.weller@chem.ox.ac.uk

■ ACKNOWLEDGMENT

We thank Prof. Judith Howard and Dr. Hazel Sparkes (University of Durham, UK), Dr. David Watkin, and Dr. Amber Thompson for discussions regarding the crystallography, the EPSRC solid-state NMR service (Durham, UK), and in particular Dr. David Apperley.

■ REFERENCES

(1) Kubas, G. J. *Metal Dihydrogen and σ-Bond Complexes*; Kluwer Academic/Plenum Publishers: New York, 2001.
(2) Brookhart, M.; Green, M. L. H.; Parkin, G. *Proc. Natl. Acad. Sci. U.S.A.* **2007**, *104*, 6908.
(3) Kubas, G. J. *Chem. Rev.* **2007**, *107*, 4152.
(4) Kubas, G. J.; Unksefer, C. J.; Swanson, B. I.; Fukushima, E. *J. Am. Chem. Soc.* **1986**, *108*, 7000.
(5) Ball, G. E.; Brookes, C. M.; Cowan, A. J.; Darwish, T. A.; George, M. W.; Kawanami, H. K.; Portius, P.; Rourke, J. P. *Proc. Natl. Acad. Sci. U. S.A.* **2007**, *104*, 6927.
(6) Cowan, A. J.; Portius, P.; Kawanami, H. K.; Jina, O. S.; Grills, D. C.; Sun, X. Z.; McMaster, J.; George, M. W. *Proc. Natl. Acad. Sci. U.S. A.* **2007**, *104*, 6933.
(7) Bernskoetter, W. H.; Schauer, C. K.; Goldberg, K. I.; Brookhart, M. *Science* **2009**, *326*, 553.
(8) Rybtchinski, B.; Milstein, D. *Angew. Chem., Int. Ed.* **1999**, *38*, 870.
(9) Jun, C. H. *Chem. Soc. Rev.* **2004**, *33*, 610.
(10) Jazzar, R. F. R.; Macgregor, S. A.; Mahon, M. F.; Richards, S. P.; Whittlesey, M. K. *J. Am. Chem. Soc.* **2002**, *124*, 4944.
(11) Sattler, A.; Parkin, G. *Nature* **2010**, *463*, 523.
(12) Gandelman, M.; Vigalok, A.; Konstantinovski, L.; Milstein, D. *J. Am. Chem. Soc.* **2000**, *122*, 9848.
(13) Goldfuss, B.; Schleyer, P. V.; Hampel, F. *J. Am. Chem. Soc.* **1996**, *118*, 12183.
(14) Tomaszewski, R.; Hyla-Kryspin, I.; Mayne, C. L.; Arif, A. M.; Gleiter, R.; Ernst, R. D. *J. Am. Chem. Soc.* **1998**, *120*, 2959.
(15) Vigalok, A.; Rybtchinski, B.; Shimon, L. J. W.; Ben-David, Y.; Milstein, D. *Organometallics* **1999**, *18*, 895.
(16) Gandelman, M.; Konstantinovski, L.; Rozenberg, H.; Milstein, D. *Chem.—Eur. J.* **2003**, *9*, 2595.
(17) Jaffart, J.; Cole, M. L.; Etienne, M.; Reinhold, M.; McGrady, J. E.; Maseras, F. *Dalton Trans.* **2003**, 4057.
(18) Summerscales, O. T.; Cloke, F. G. N.; Hitchcock, P. B.; Green, J. C.; Hazari, N. *Science* **2006**, *311*, 829.
(19) Harvey, B. G.; Mayne, C. L.; Arif, A. M.; Ernst, R. D. *J. Am. Chem. Soc.* **2005**, *127*, 16426.
(20) Madison, B. L.; Thyme, S. B.; Keene, S.; Williams, B. S. *J. Am. Chem. Soc.* **2007**, *129*, 9538.
(21) Boulho, C.; Keys, T.; Coppel, Y.; Vendier, L.; Etienne, M.; Locati, A.; Bessac, F.; Maseras, F.; Pantazis, D. A.; McGrady, J. E. *Organometallics* **2009**, *28*, 940.
(22) Scheins, S.; Messerschmidt, M.; Gembicky, M.; Pitak, M.; Volkov, A.; Coppens, P.; Harvey, B. G.; Turpin, G. C.; Arif, A. M.; Ernst, R. D. *J. Am. Chem. Soc.* **2009**, *131*, 6154.
(23) Harvey, B. G.; Arif, A. M.; Ernst, R. D. *J. Organomet. Chem.* **2006**, *691*, 5211.
(24) Boulho, C. d.; Keys, T.; Coppel, Y.; Vendier, L.; Etienne, M.; Locati, A.; Bessac, F.; Maseras, F.; Pantazis, D. A.; McGrady, J. E. *Organometallics* **2009**, *28*, 940.
(25) An Ir(I) complex initially described as having a C−C σ interaction has since been re-evaluted as simply having relatively close nonbonding contacts but no lengthening of the C−C bond: Maseras, F; Crabtree, R. H. *Inorg. Chim. Acta* **2004**, *357*, 345.
(26) An example of a Si−Si σ-complex has also been reported: Chen, W.; Shimada, S.; Tanaka, M. *Science* **2002**, *295*, 308. Nikonov, G. I. *Angew. Chem., Int. Ed.* **2003**, *42*, 1335.
(27) Brayshaw, S. K.; Green, J. C.; Kociok-Kohn, G.; Sceats, E. L.; Weller, A. S. *Angew. Chem., Int. Ed.* **2006**, *45*, 452.
(28) Brayshaw, S. K.; Sceats, E. L.; Green, J. C.; Weller, A. S. *Proc. Natl. Acad. Sci. U.S.A.* **2007**, *104*, 6921.
(29) Kubas, G. J. *Proc. Natl. Acad. Sci. U.S.A.* **2007**, *104*, 6901.
(30) Taw, F. L.; Mellows, H.; White, P. S.; Hollander, F. J.; Bergman, R. G.; Brookhart, M.; Heinekey, D. M. *J. Am. Chem. Soc.* **2002**, *124*, 5100.
(31) Gilbert, T. M.; Bergman, R. G. *J. Am. Chem. Soc.* **1985**, *107*, 3502.
(32) Bernskoetter, W. H.; Hanson, S. K.; Buzak, S. K.; Davis, Z.; White, P. S.; Swartz, R.; Goldberg, K. I.; Brookhart, M. *J. Am. Chem. Soc.* **2009**, *131*, 8603.
(33) Gunay, A.; Jones, W. D. *J. Am. Chem. Soc.* **2007**, *129*, 8729.
(34) Escudero, D.; Weisheit, T.; Weigand, W.; Gonzalez, L. *Dalton Trans.* **2010**, *39*, 9505.

(35) Monreal, M. J.; Diaconescu, P. L. *J. Am. Chem. Soc.* **2010**, *132*, 7676.
(36) Evans, M. E.; Li, T.; Jones, W. D. *J. Am. Chem. Soc.* **2010**, *132*, 16278.
(37) Periana, R. A.; Bergman, R. G. *J. Am. Chem. Soc.* **1986**, *108*, 7346.
(38) Wu, Y.; Jin, L.; Xue, Y.; Lee, I. M.; Kim, C. K. *J. Comput. Chem.* **2010**, *31*, 2248.
(39) Khawam, A.; Flanagan, D. R. *J. Phys. Chem. B.* **2006**, *110*, 17315.
(40) Schrock, R. R.; Osborn, J. A. *J. Am. Chem. Soc.* **1971**, *93*, 3089.
(41) Acton, N.; Roth, R. J.; Maier, C. A.; Katz, T. J.; Frank, J. K.; Paul, I. C. *J. Am. Chem. Soc.* **1972**, *94*, 5446.
(42) Bezman, S. A.; Bird, P. H.; Fraser, A. R.; Osborn, J. A. *Inorg. Chem.* **1980**, *19*, 3755.
(43) Shatruk, M.; Dragulescu-Andrasi, A.; Chambers, K. E.; Stoian, S. A.; Bominaar, E. L.; Achim, C.; Dunbar, K. R. *J. Am. Chem. Soc.* **2007**, *129*, 6104.
(44) Braga, D. *Chem. Rev.* **1992**, *92*, 633.
(45) Farrugia, L. J.; Senior, A. R. M.; Braga, D.; Grepioni, F.; Orpen, A. G.; Crossley, J. G. *J. Chem. Soc., Dalton Trans.* **1996**, 631.
(46) Farrugia, L. J.; Gillon, A. L.; Braga, D.; Grepioni, F. *Organometallics* **1999**, *18*, 5022.
(47) Silvernail, N. J.; Barabanschikov, A.; Sage, J. T.; Noll, B. C.; Scheidt, W. R. *J. Am. Chem. Soc.* **2009**, *131*, 2131.
(48) Rosenfield, R.; Tureblood, K.; Dunitz, J. *Acta Crystallogr.* **1978**, *A34*, 828.
(49) DFT calculations were carried out using the Gaussian suite with the B3LYP functional. A GEN basis set employed with 6-31G(d,p) for H, C, and P and SDD for Ir. Full details are given in the Supporting Information.
(50) This very low energy barrier connecting **3a** and **3b** has analogy with the situation found in "compressed dihydride" complexes of iridium (see ref 52), which have extremely flat potential energy surfaces connecting dihydrogen and dihydride structures.
(51) Rh(V) complexes see: McBee, J. L.; Escalada, J.; Tilley, T. D. *J. Am. Chem. Soc.* **2009**, *131*, 12703 and references therein.
(52) Pons, V.; Heinekey, D. M. *J. Am. Chem. Soc.* **2003**, *125*, 8428.
(53) A related rapid equilibration of Ir−dihydride and Ir−elogonated dihydrogen isomers in $IrH_2(2,6\text{-}(^tBu_2PO)_2C_6H_3)$ has also been reported: Göttker-Schnetmann, I.; Heinekey, D. M.; Brookhart, M. *J. Am. Chem. Soc.* **2006**, *128*, 17114.
(54) Gelabert, R.; Moreno, M.; Lluch, J. M.; Lledós, A.; Pons, V.; Heinekey, D. M. *J. Am. Chem. Soc.* **2004**, *126*, 8813.
(55) Mort, B. C.; Autschbach, J. *J. Am. Chem. Soc.* **2006**, *128*, 10060.
(56) Gelabert, R.; Moreno, M.; Lluch, J. M.; Lledós, A.; Heinekey, D. M. *J. Am. Chem. Soc.* **2005**, *127*, 5632.
(57) Dziallasa, M.; Höhna, A.; Werner, H. *J. Organomet. Chem.* **1987**, *330*, 207.